Mon. Not. R. Astron. Soc. **000**, 000–000 (0000) Printed 21 May 2010 (MN LATEX style file v2.2)

Molecular Gas in SAURON Early-Type Galaxies: Detection of ^{13}CO and HCN Emission⋆

M. Krips,[1]† A. F. Crocker,[2] M. Bureau,[2] F. Combes,[3] and L. M. Young[4]
[1]*Institut de Radio Astronomie Millimetrique (IRAM), Domaine Universitaire, 300 rue de la Piscine, 38406 Saint Martin d'Hères, France*
[2]*Sub-Department of Astrophysics, University of Oxford, Denys Wilkinson Building, Keble Road, Oxford OX1 3RH, U.K.*
[3]*Observatoire de Paris, LERMA, 61 Av. de l'Observatoire, 75014 Paris, France*
[4]*Physics Department, New Mexico Institute of Mining and Technology, Socorro, NM 87801, U.S.A.*

Received ; accepted

ABSTRACT

In a pilot project to study the relationship between star formation and molecular gas properties in nearby normal early-type galaxies, we have obtained observations of dense molecular gas tracers in the four galaxies of the SAURON sample with the strongest ^{12}CO emission. We used the Institut de Radio Astronomie Millimetrique (IRAM) 30m telescope 3 and 1 mm heterodyne receivers to observe the ^{13}CO(J=1–0), ^{13}CO(J=2–1), HCN(J=1–0) and HCO$^+$(J=1–0). We report the detection of ^{13}CO emission in **all four** SAURON sources and HCN emission in three sources, while no HCO$^+$ emission was found to our detection limits **in any** of the four galaxies. We find that the ^{13}CO/^{12}CO ratios of three SAURON galaxies are somewhat higher than those in galaxies of different Hubble types. The HCN/^{12}CO and HCN/^{13}CO ratios of all four SAURON galaxies resemble those of nearby Seyfert and dwarf galaxies with normal star formation rates, rather than those of starburst galaxies. The HCN/HCO$^+$ ratio is found to be relatively high (i.e., >1) in the three SAURON galaxies with detected HCN emission, mimicking the behaviour in other star-forming galaxies but being higher than in starburst galaxies. When compared to most galaxies, it thus appears that ^{13}CO is enhanced (relative to ^{12}CO) in three out of four SAURON galaxies and HCO$^+$ is weak (relative to HCN) in three out of three galaxies.

All three galaxies detected in HCN follow the standard HCN–infrared luminosity and dense gas fraction–star formation efficiency correlations. As already suggested by ^{12}CO observations, when traced by infrared radiation, star formation in the three SAURON galaxies thus appears to follow the same physical laws as in galaxies of different Hubble types. The star formation rate and fraction of dense molecular gas however do not reach the high values found in nearby starburst galaxies, but rather resemble those of nearby normal star-forming galaxies.

Key words: galaxies: elliptical and lenticular, cD – galaxies: evolution – galaxies: ISM – galaxies: kinematics and dynamics – galaxies: structure – Radio lines: galaxies

1 INTRODUCTION

Over the last twenty years, growing evidence has accumulated that nearby early-type galaxies (E/S0s) are not always devoid of molecular gas, and can even harbour a substantial amount of it (e.g., Lees et al. 1991; Wiklind, Combes & Henkel 1995; Bettoni, Galletta & García-Burillo 2003; Sage, Welch & Young 2007; Combes, Young & Bureau 2007; Young et al. 2010), often settled in a regularly rotating disc (e.g., Young 2002, 2005; Young, Bureau & Cappellari 2008; Crocker et al. 2008, 2009, 2010). Interestingly, not all early-type galaxies with a substantial amount of molecular gas show obvious signs of (current) star formation (SF; e.g., Crocker et al. 2008, 2009, 2010; Young et al. 2008). However, the converse is generally true (e.g., Jeong et al. 2009), and the $\gtrsim$ 30 per cent fraction of SF objects within the nearby early-type galaxy population (e.g., Yi et al. 2005) appears to be superficially consistent with their $\approx$ 25 per cent CO detection rate (e.g., Sage & Welch 2006; Sage et al. 2007; Combes et al. 2007; Young et al. 2010). This fact raises many as yet unanswered questions: how is the (current) SF ignited in early-type galaxies? Is SF coupled to the molecular discs, i.e. do all molecular gas discs form stars? Does SF only take place in the densest regions, perhaps ill-traced by the ^{12}CO lines used in most surveys? How, if at all, does the morphology of the molecular discs and the physical characteristics of the molecular gas correlate with the ages

⋆ Based on observations carried out with the IRAM 30m telescope. IRAM is supported by INSU/CNRS (France), MPG (Germany) and IGN (Spain).
† E-mail: krips@iram.fr

Table 1. Basic parameters of the four SAURON galaxies.

NGC	RA(J2000) (hh:mm:ss.s)	DEC(J2000) (dd:mm:ss)	$V_\odot$ (km s^{-1})	D (Mpc)	Activity Type
3032	09:52:08.2	+29:14:10	1533	21.7	H II
4150	12:10:33.6	+30:24:06	226	13.7	none
4459	12:29:00.0	+13:58:43	1210	16.3	H II+L
4526	12:34:03.0	+07:41:57	550	16.3	none

Notes: Coordinates, distances, velocities and activity types are taken from the NASA/IPAC Extragalactic Database (NED). Galaxy types: L=LINER, H II=star formation bursts.

of the stars? In order to answer some of these questions, it is essential to study the spatially- and kinematically-resolved properties of the stellar populations, as well as those of the molecular gas in early-type galaxies (E/S0). CO emission can also easily trace signs of gravitational interactions or other dynamical perturbations that can help to understand how star formation is induced.

Observations of a sample of 48 nearby E/S0 galaxies have been carried out with a custom-designed panoramic optical integral-field spectrograph (Bacon et al. 2001) within the framework of the SAURON project. A description of the sample and illustrative results can be found in de Zeeuw et al. (2002). Results include the detection of kinematic misalignments, twists and decoupled cores as well as central discs in roughly half of the sources (Emsellem et al. 2004; Krajnović et al. 2008). Information on the ionized gas (distribution, kinematics and ionisation; Sarzi et al. 2006, 2010) and the age, metallicity and alpha-element enhancement of the stellar populations (Kuntschner et al. 2006, 2010) are also available. The specific angular momentum of the galaxies appears to be a dominant factor in their evolution (Emsellem et al. 2007; Cappellari et al. 2007), and all CO detections are found in fast-rotating systems (Young et al. 2010).

In order to study star formation in the SAURON sources and understand the various phenomena observed in the stellar and ionised gas data, observations looking for central molecular gas in the nearby SAURON E/S0 galaxies were obtained by Combes et al. (2007). ^{12}CO emission was detected in 12 of 43 galaxies observed with the Institut de Radio Astronomie Millimetrique (IRAM) 30m telescope, suggesting typical gas masses in a range between a few 10^6 to 10^8 M$_\odot$. Combes et al. (2007) further found that the amount of molecular gas in the galaxies correlates with their far-infrared (FIR) luminosities, an often-used indicator of star formation. The gas-rich sources show the most pronounced star formation, as for normal star-forming spiral galaxies. However, the lack of correlations between the molecular gas and most stellar properties suggests that the molecular gas is largely unrelated to the old, pre-existing stellar population, and might have been externally accreted, as a result for instance of a merger or interaction event (Combes et al. 2007).

However, as ^{12}CO emission has been found to be a rather unreliable tracer of the dense gas where star formation takes place (e.g., Gao & Solomon 2004a,b), as a pilot study we focus here on the volume and/or column density tracers HCN, HCO$^+$ and ^{13}CO in the four SAURON galaxies with the brightest ^{12}CO emission. Basic parameters of these four sources are given in Table 1. They form an interesting subset of the SAURON sample as they nicely populate the two main evolutionary groups: i) those with a more 'troubled' recent past, likely involving accretion and/or minor interactions with other galaxies (NGC 3032 and NGC 4150); and ii) those with a more peaceful immediate past dominated by secular evolution (NGC 4459 and NGC 4526). The first group appears to harbor a large fraction of widely distributed young stars while the second group possesses a lower young stellar fraction that is spatially limited to the center (Kuntschner et al. 2010). Additionally, NGC 3032 shows signs that its young stars have a lower metallicity than its bulk stellar population. Nevertheless, only NGC 3032 and NGC 4459 show signs of circumnuclear activity both in the form of H II regions, indicative of star formation bursts, and, in the case of NGC 4459 also in the form of a low-ionization nuclear emission region (LINER) nucleus.

The paper is organised as follows. Section 2 presents the observations. Section 3 consists of the results and a discussion of the data and their trends. Finally, section 4 summarizes our findings and conclusions.

2 OBSERVATIONS

Using the IRAM 30m telescope at Pico Veleta, Spain, in August 2008 and **April 2010**, we observed the ^{13}CO(J=1–0), ^{13}CO(J=2–1), HCN(J=1–0) and HCO$^+$(J=1–0) lines in the centres of our four target galaxies. In 2009, we used the AB set of receivers with the 1 and 4 MHz backends at 3 and 1.4 mm (89–110 GHz and 22 GHz), respectively, **while we used the Eight Mixer Receiver (EMIR) with the Wideband Line Multiple Autocorrelator (WILMA) backend in 2010**. The weather was exceptionally good in **both years**, with a precipitable water vapour at 3 mm of $\leqslant$ 5 mm during $\approx$ 90 per cent of the time and 5–15 mm during $\approx$ 10 per cent of the time, corresponding to system temperatures $T_{\rm sys}$ = 100–200 K at 3 mm and $\approx$ 300 K at 1.4 mm. We discarded all 1.4 mm data obtained at 3 mm precipitable water vapour of 5–15 mm while we kept the corresponding 3 mm data as the system temperatures were still in an acceptable range (i.e., Tsys$\simeq$250 K). We spent 2–5 hr on source per target and frequency, resulting in an rms noise level (in T$_{\rm mb}$ scale) of $\approx$ 0.5–1 mK for HCN and HCO$^+$ (binned to $\approx$ 30 km s^{-1}) and of $\approx$ 2–3 mK for ^{13}CO (binned to $\approx$ 20 km s^{-1}). Pointing and focus tests were carried out every 1.5–2 hr on a nearby planet ($<$ 30°; Mars and/or Saturn) or a nearby strong quasar ($<$ 10°; 0924+392). The pointings were consistent with each other within $\approx$ 1–3 arcsec throughout the observations. This is entirely sufficient given the beam sizes (half power beam width, HPBW) of 27 arcsec for HCN(J=1–0) and HCO$^+$(J=1–0), 22 arcsec for ^{13}CO(J=1–0) and 11 arcsec for ^{13}CO(J=2–1).

To remove the continuum from each spectrum, a baseline of polynomial order 0 or 1 was fit to the line-free regions of each scan and subtracted, and the scans were thereafter averaged. We measured the peak intensities, central velocities, full width half maxima (FWHM) and velocity-integrated fluxes of the detected lines by fitting Gaussian profiles to the data. Some of the lines clearly exhibit multiple peaks, so we compared line intensities obtained from both multiple and single Gaussian fits. As the (summed) line intensities agreed well with each other, we will use the values from the single Gaussian fits in the following.

Antenna temperatures ($T_{\rm a}^\star$) have been converted to main beam temperatures ($T_{\rm mb}$) by dividing the antenna temperatures by $\eta \equiv B_{\rm eff}/F_{\rm eff}$, where $B_{\rm eff}$ and $F_{\rm eff}$ are the beam and forward efficiencies, respectively (i.e., $T_{\rm mb} = T_{\rm a}^\star/\eta$; η = 0.78/0.95 = 0.82 for HCN and HCO$^+$, η = 0.75/0.95 = 0.79 for ^{13}CO(J=1–0) and η = 0.55/0.91 = 0.60 for ^{13}CO(J=2–1)). To convert the measured brightness temperatures ($T_{\rm mb}$[K]) to fluxes (S[Jy]) via S[Jy]= $f_{\rm conv}\, T_{\rm mb}$[K], the following conversion factors must be used: $f_{\rm conv}$ =

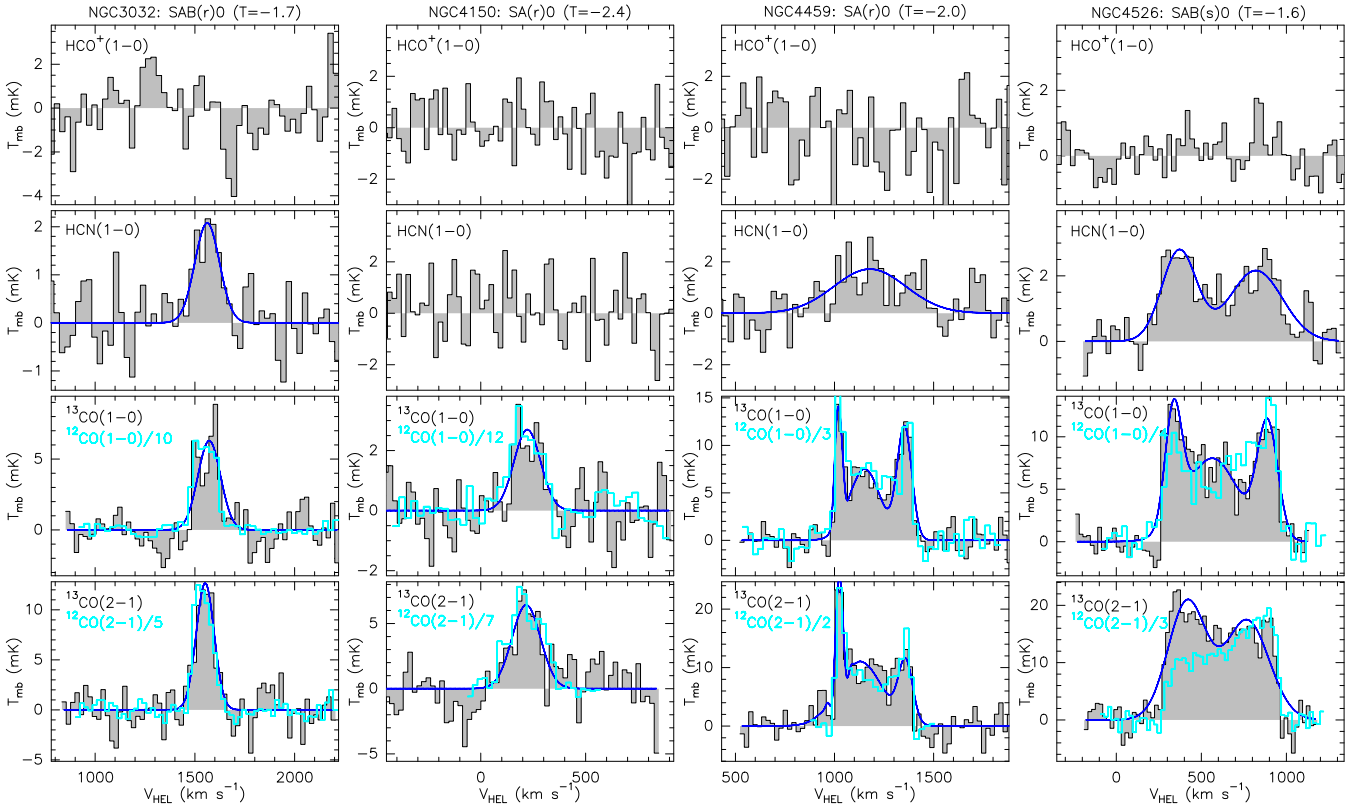

Figure 1. Emission line spectra of the four SAURON early-type galaxies observed. From top to bottom in each panel: HCO^+(J=1–0), HCN(J=1–0), ^{13}CO(J=1–0) and ^{13}CO(J=2–1). From left to right: NGC 3032, NGC 4150, NGC 4459 and NGC 4526. The ^{13}CO emission is overlaid with the spectra of the ^{12}CO emission (*cyan*) from Combes et al. (2007), scaled down to match the ^{13}CO line emission; the scaling factors are indicated in the respective spectra. The (single, dual, triple) Gaussian fits to the line spectra are plotted in dark blue.

Table 2. Properties of the molecular line spectra.

Line Parameters[a]	^{12}CO(J=1–0) (CYB07)	^{12}CO(J=2–1) (CYB07)	^{13}CO(J=1–0) (this paper)	^{13}CO(J=2–1) (this paper)	HCN(J=1–0) (this paper)	HCO^+(J=1–0)[b] (this paper)
NGC3032:						
I (K km s^{-1})	9.3±0.3	7.9±0.2	0.9±0.1	1.4±0.2	0.32±0.09	<0.2
$< v_\odot >$ (km s^{-1})	1549±2	1537±2	1571±10	1561±10	1571±13	
Δv (km s^{-1})	129±4	103±3	130±14	104±10	160±30	
NGC4150:						
I (K km s^{-1})	6.1±0.5	13.2±0.5	0.4±0.1	1.1±0.2	<**0.2**	<**0.2**
$< v_\odot >$ (km s^{-1})	204±7	200±3	221±14	226±12		
Δv (km s^{-1})	158±14	189±8	150±30	160±30		
NGC4459:						
I (K km s^{-1})	10.9±0.5	14.3±0.5	3.2±0.2	4.9±0.4	0.8±0.1	<0.7
$< v_\odot >$ (km s^{-1})	1169±9	1176±8	1194±22	1179±40	1140±20	
Δv (km s^{-1})	477±16	405±15	390±20	380±20	440±70	
NGC4526:						
I (K km s^{-1})	23.8±0.8	37.4±0.7	6.0±0.2	11±0.4	1.6±0.1	<0.7
$< v_\odot >$ (km s^{-1})	697±2	695±5	605±30	600±30	606±40	
Δv (km s^{-1})	650±23	533±11	687±26	677±27	760±50	

Notes: [a]Line properties have been obtained by fitting a single Gaussian to the data from Combes et al. (2007) and this paper; $I \equiv \int T_{\rm mb}\, dv$ is the velocity-integrated line intensity; $< v_\odot >$ is the mean (central) heliocentric velocity; Δv is the velocity width (FWHM). [b] Determined from 3σ upper limits from spectrum at ∼100 km s^{-1} spectral resolution assuming the same FWHM as found for the HCN(J=1–0) or ^{13}CO(J=1–0) line.

4.9 Jy K^{-1} for HCN(J=1–0) and HCO$^+$(J=1–0), $f_{\rm conv}$ = 5.0 Jy K^{-1} for ^{13}CO(J=1–0) and $f_{\rm conv}$ = 5.8 Jy K^{-1} for ^{13}CO(J=2–1).

3 RESULTS AND DISCUSSION

We detected ^{13}CO(J=1–0) and ^{13}CO(J=2–1) emission in four out of four sources and HCN(J=1–0) emission **in three out of four** sources, while HCO$^+$ emission is undetected in **all four sources**. The spectra of the individual lines for each galaxy are plotted in Fig. 1. We also overlay the ^{12}CO emission from Combes et al. (2007) on our ^{13}CO detections for a direct comparison. The line parameters obtained from Gaussian fits to the data are listed in Table 2 and compared to the ^{12}CO data from Combes et al. (2007). All the line profiles appear to agree well with each other for each individual galaxy. Only the ^{13}CO(J=2–1) line in NGC4459 and NGC4526 shows some asymmetry, with a stronger blueshifted peak, but this can probably be attributed to the smaller beam at 1.4 mm and thus a different beam filling at 3 and 1.4 mm. While the ^{13}CO line emission in all galaxies except NGC 4526 strongly resembles that of ^{12}CO, the ^{13}CO(J=2–1) line in NGC 4526 differs from that of ^{12}CO(J=2–1). This is most likely due to a slightly different pointing during the two observations, which will be considered for the line ratios in the following discussion. It also indicates that the emission in NGC 4526 (and probably NGC 4459) is slightly larger than the beam size at 1 mm. The fitted heliocentric velocities also agree with each other for all galaxies except NGC 4526, where the measured velocities differ from each other by $\approx$90 km s^{-1}. However, this difference can be explained by the Gaussian fit to the asymmetric line profile of the ^{12}CO emission done in Combes et al. (2007), which favours the stronger redshifted peak and thus shifts the line centre towards higher velocities (see also Fig. 1). If one calculates the central velocities from the full widths at zero maximum (FWZM), one finds a more consistent value of $\approx$ 620 km s^{-1}.

We calculated line ratios between the total of 6 molecular lines observed for each galaxy (see Table 3 and Fig. 2). To avoid systematic errors due to beam dilution effects, we only determined line ratios at similar frequencies, i.e. observed with similar beam sizes. Please note that we consider the line ratio between the ^{13}CO(J=2–1) and ^{12}CO(J=2–1) line emission as uncertain given their different line profiles (see discussion in the previous paragraph). The line ratios are compared to those in galaxies of different Hubble types in Table 3 and Figure 2. The list of galaxies of different Hubble types should be regarded as representative of each type and does not attempt to be complete. We explicitly state the region of each galaxy where the line ratios have been taken. This is especially important for the very nearby galaxies such as M33, M31 and the dwarf galaxies, for which the observations already resolve giant molecular clouds (GMCs) and cannot be regarded as averaging over the central regions of each galaxy. In addition, previous studies indicate that molecular line ratios can vary significantly within a galaxy (e.g., Wilson, Walker & Thornley 1997; Helfer & Blitz 1997; Brouillet et al. 2005; Krips et al. 2007), especially for galaxies with an active galactic nucleus (AGN). NGC 1068 and NGC 6951 are prominent examples of completely different chemistry and excitation conditions of the molecular gas close to the AGN and in the (star formation-dominated) large-scale spiral arms (e.g., Sternberg, Genzel & Tacconi 1994; Krips et al. 2007, 2008).

Although the ^{13}CO/^{12}CO line ratios appear to be quite similar among galaxies of different Hubble types, with values in general around 0.1-0.2, certain trends can nevertheless be identified. While the starburst galaxies and (U)LIRGs seem to populate the lower end of the line ratio distribution (with values $\lesssim$0.1), three of the four SAURON galaxies lie at the higher end of it, with values larger than 0.2 in at least one of the two transitions (see Fig. 2). Casoli et al. (1992) suggest that the low ^{13}CO/^{12}CO ratios in starburst galaxies are not a consequence of excitation conditions and/or optical depth effects, but are rather due to an actual change in the ^{13}CO/^{12}CO abundance ratio itself, either by overabundant ^{12}CO or underabundant ^{13}CO. As numerous new massive stars are formed during a starburst, the interstellar medium will be preferentially enriched by nucleosynthesis of ^{12}C, whereas ^{13}C remains unaffected. Also, at least in the case of a merger-induced starburst, the infall of large-scale gas to the centre will result in a dilution of the central ^{13}CO gas, as the infalling gas is poor in ^{13}CO. As for the high ^{13}CO/^{12}CO line ratios in three of the four SAURON galaxies, optical depth may well play a significant role, with e.g., optically thick ^{12}CO emission.

The HCN/^{13}CO and HCN/^{12}CO ratios are similar to those of the (star formation-dominated) central regions of nearby Seyfert and spiral galaxies as well as those of GMCs in dwarf galaxies (see Fig. 2), but they are quite different from (i.e., smaller than those of) nearby starburst galaxies and the (AGN-dominated) circumnuclear discs (CNDs) of some Seyfert galaxies (CNDs being smaller than the central regions considered in the Seyferts).

The SAURON early-type galaxies stand out most when considering the HCN/HCO$^+$ ratio, varying most significantly again not as a function of Hubble type but rather of activity type (Fig. 2; see also Krips et al. 2008). Here, the SAURON galaxies strongly resemble the (AGN-dominated) circumnuclear regions of some Seyfert (e.g. NGC 1068, NGC 6951 and M51) and some (ultra-)luminous infrared galaxies ((U)LIRGs). However, they differ from most starburst and the dwarf galaxies (at least the Magellanic Clouds) as well as Centaurus A (Cen A). Nevertheless, because of the high HCN/^{13}CO and HCN/^{12}CO ratios of these Seyfert galaxies, the high HCN/HCO$^+$ ratios in the SAURON early-type galaxies probably have a different origin than that in the Seyferts. While the high HCN/HCO$^+$ ratios in the Seyfert galaxies are believed to be a consequence of enhanced HCN emission (e.g., Sternberg et al. 1994; Usero et al. 2004; Krips et al. 2007, 2008), those in the SAURON galaxies appear to be due to lowered HCO$^+$ emission instead.

HCO$^+$ is known to be enhanced over HCN in galaxies with strong starburst activity, with a likely dependence on the age of the star formation burst, i.e. the older the star formation burst the lower the HCN/HCO$^+$ ratio (see the examples of the evolved starburst galaxy M82 and the young starburst NGC 6946; Krips et al. 2008 and references therein). This effect is thought to be a consequence of the increased rate of supernova explosions and/or the increased importance of photo-dissociation regions (PDRs) in more evolved starburst galaxies. The high HCN/HCO+ ratios observed here in the four SAURON targets may thus indicate that supernova explosions (or, equally, PDRs) only play a minor role in the gas chemistry of these early-types.

It is interesting to note that the molecular line ratios of most of the SAURON early-type galaxies are not very similar to those of the elliptical galaxy Cen A. Cen A rather seems to favour line ratios close to those of the dwarf galaxies in our list. This is not entirely surprising however as the molecular gas in Cen A, mostly located in the minor-axis dust lane, has almost certainly been captured during a merger event with a gas-rich dwarf or small disc galaxy (e.g., Malin, Quinn & Graham 1983).

When comparing the HCN luminosity to the IR luminosity (a measure of star formation; see Fig. 3), one finds that the four SAURON sources nicely follow the IR–HCN correlation of star-

forming galaxies, firmly extending the relation to lower luminosities. Plotting both of these luminosities (IR and HCN) normalized by the ^{12}CO luminosity (thus measuring star formation efficiency against dense gas fraction), our early-type galaxies again lie comfortably on the relation (e.g., Solomon et al. 1992; Gao & Solomon 2004a,b), having both relatively average dense gas fractions and star formation efficiencies (SFEs). This suggests that most of the star formation in these four SAURON early-type galaxies is taking place in dense gas regions, as in other nearby (spiral) galaxies. The dense gas fraction is however lower than what is found in truly starbursting galaxies.

4 SUMMARY AND CONCLUSIONS

We detected significant ^{13}CO in four out of four and HCN emission **in three out of four** SAURON early-type galaxies, while no HCO$^+$ emission was found in any of the four sources. We find some pronounced differences in the line ratios of the SAURON galaxies when compared to other nearby galaxies of different Hubble and activity types. In particular, ^{13}CO/^{12}CO appears slightly enhanced in three SAURON galaxies compared to other galaxy types. This may indicate different molecular gas excitation conditions and/or chemistry in these sources. The closest resemblance to our four nearby SAURON galaxies is found in nearby star-forming galaxies, including Seyferts and dwarfs. This and the pronounced differences with starburst galaxies suggest that the four SAURON galaxies exhibit star-formation rates and efficiencies more similar to quiescent, normal star-forming galaxies than to starburst galaxies, and that they do not reach the high dense molecular gas fraction found in starbursts. Also, according to the high (>1) HCN/HCO$^+$ ratios, PDRs and/or supernovae explosions do not seem to play an important role in the chemistry of the molecular gas in our four targets.

The three SAURON galaxies observed in HCN nicely follow the same physical laws concerning star formation and dense molecular gas as other galaxies, at least when infrared radiation is used as the star formation tracer.

Although the four SAURON galaxies studied in this paper form a nice subset of the SAURON sample with respect to their general characteristics, they are not equally representative with respect to their molecular gas properties. They have been chosen for their strong ^{12}CO emission and could thus in principal be extreme cases within the sample. Follow-up observations of the ^{13}CO, HCN and HCO$^+$ emission in a much larger sample of nearby early-type galaxies are currently underway based on the success of this pilot study. These will eventually allow us to confirm (or discard) the trends found in this pilot project and put them on a sounder statistical basis.

ACKNOWLEDGMENTS

We thank the IRAM staff at the IRAM 30 m telescope at Pico Veleta for their help during the observations. We would like to thank various members of the SAURON team for useful discussions throughout this project and the referee for a thorough review of the paper. We acknowledge the usage of the HyperLeda database (Paturel et al. 2003, http://leda.univ-lyon1.fr). This research has made use of the NASA/IPAC Extragalactic Database (NED) which is operated by the Jet Propulsion Laboratory, California Institute of Technology, under contract with the National Aeronautics and Space Administration.

REFERENCES

Aalto, S., Booth, R. S., Black, J. H., & Johansson, L. E. B., 1995, A&A, 300, 369
Baan, W.A., Henkel, C., Loenen, A.F., Baudry, A., Wiklind, T., 2008, A&A, 477, 747
Bacon R., et al., 2001, MNRAS, 326, 23
Bettoni D., Galletta, G., García-Burillo S., 2003, A&A, 405, 5
Bolatto A. D., Israel F. P., Martin Ch. L., 2005, ApJ, 633, 210
Brouillet N., Muller S., Herpin F., Braine J., Jacq T., 2005, A&A, 429, 153
Cappellari M., et al., 2007, MNRAS, 379, 418
Casoli, F., Dupraz, C., & Combes, F., 1992, A&A, 264, 55
Chin Y.-N., Henkel C., Whiteoak J. B., Millar T. J., Hunt M. R., Lemme C., 1997, A&A, 317, 548
Combes F., Young L. M., Bureau M., 2007, MNRAS, 377, 1795
Crocker A. F., Bureau M., Young L. M., Combes F., 2008, MNRAS, 386, 1811
Crocker A. F., Jeong H., Komugi S., Combes F., Bureau M., Young L. M., Yi S., 2009, MNRAS, 393, 1255
Crocker A. F., Bureau M., Young L. M., Combes F., 2010, MNRAS, submitted
de Zeeuw P. T. et al., 2002, MNRAS, 329, 513
Emsellem E., et al., 2004, MNRAS, 352, 721
Emsellem E., et al., 2007, MNRAS, 379, 401
Gao Y., Solomon P. M., 2004a, ApJS, 152, 63
Gao Y., Solomon P. M., 2004b, ApJ, 606, 271
García-Burillo S., Combes F., Usero A., Gracià-Carpio J., Journal of Physics: Conference Series, Volume 131, Proceedings of "The Universe Under the Microscope - Astrophysics at High Angular Resolution", eds. R. Schoedel, A. Eckart, S. Pfalzner, E. Ros, p. 01203
Glenn, J.; Hunter, T.R., 2001, ApJS, 135, 177
Heikkilä A., Johansson L. E. B., Olofsson H., 1999, A&A, 344, 817
Helfer T. T., Blitz L., 1997, ApJ, 478, 162
Henkel, C., Whiteoak, J.B., & Mauersberger, R., 1994, A&A, 284, 17
Israel F. P., 2009a, A&A, 493, 525
Israel F. P., 2009b, A&A, 506, 689
Israel F. P., 2001, A&A, 371, 433
Israel F. P., Tilanus R. P. J., Baas F., 2006, A&A, 445, 907
Israel, F. P.; Baas, F., 1999, A&A, 351, 10
Jeong H., et a., 2009, MNRAS, in press
Krajnović D., et al., MNRAS, 2008, 390, 93
Krips M., Neri R., García-Burillo S., Martín S., Combes F., Gracià-Carpio J., Eckart A., 2008, ApJ, 677, 26
Krips M., Neri R., García-Burillo S., Combes F., Schinnerer E., Baker A. J., Eckart A., Boone F., Hunt L., Leon S., Tacconi L. J., 2008b, A&A, 468, L63
Kuntschner H., et al., MNRAS, 2006, 369, 497
Kuntschner H., et al., MNRAS, 2010, in press.
Lees J. F., Knapp G. R., Rupen M. P., Phillips T. G., 1991, ApJ, 379, 177
Malin D. F., Quinn P. J., Graham J. A, 1983, ApJ, 272, L5
Matsushita S., Kawabe R., Matsumoto H., Tsuru T. G., Kohno K., Morita K.-I., Okumura S. K., Vila-Vilaró B., 2000, ApJ, 545, L107
Meier, D.S.; Turner, J.L.; Hurt, R.L., 2008, ApJ, 675, 281
Nguyen, Q.-Rieu; Jackson, J.M.; Henkel, Ch.; Truong, B.; Mauersberger, R.,1992, ApJ, 399, 521
Paglione T. A. D., Wall W. F., Young J. S., Heyer M. H., Richard

Table 3. Molecular line ratios for a representative set of nearby galaxies covering the Hubble sequence and different activity types.

Source	Activity Type[a]	$\frac{^{13}CO(J=1-0)}{^{12}CO(J=1-0)}$	$\frac{^{13}CO(J=2-1)}{^{12}CO(J=2-1)}$	$\frac{HCN(J=1-0)}{^{13}CO(J=1-0)}$	$\frac{HCN(J=1-0)}{^{12}CO(J=1-0)}$	$\frac{HCN(J=1-0)}{HCO^+(J=1-0)}$	Ref[b]	Region[c]
			Ellipticals: $-6 \leqslant T \leqslant -4$					
Cen A	Sy2	∼0.07	∼0.08	∼0.9	∼0.06	∼0.6[d]	(1)	Centre
		∼0.1	∼0.09	∼0.2	∼0.02	–	(1)	Dust Lane
			Sauron (S0): $-4 < T \leqslant 0$					
NGC 3032	H II	0.09±0.01	0.20±0.02	0.36±0.07	0.03±0.01	>1.7	(2)	Centre
NGC 4150	NONE	0.07±0.01	0.08±0.01	<**0.5**	<**0.03**	–	(2)	Centre
NGC 4459	H II+L	0.30±0.02	0.34±0.02	0.23±0.03	0.07±0.01	>1.1	(2)	Centre
NGC 4526	NONE	0.26±0.01	∼0.3	0.35±0.02	0.09±0.01	>2.3	(2)	Centre
			Seyferts: $0 < T < +8$					
NGC 1068⋆	Sy2	0.09±0.02	0.06±0.01	1.6±0.6	0.13±0.02	1.7±0.2	(3,6)	Centre
		∼0.02	0.062±0.002	∼80	∼1.4	∼1.4	(4,19)	CND[d]
NGC 2237	?	∼0.1	–	0.41±0.07	0.04±0.01	–	(4,5)	Centre
NGC 3079	Sy2/L	0.06±0.01	0.07±0.01	0.6±0.2	0.039±0.09	>5	(6,23)	Centre
NGC 3627	Sy2/L	∼0.06	–	∼1.1	∼0.07	1.0±0.1	(3,8)	Centre
NGC 3628	L+H II	0.12±0.02	0.10±0.02	0.34±0.09	0.027±0.007	1.6±0.5	(22,26)	Centre
NGC 3982	Sy1.9+H II	0.07±0.01	–	0.32±0.08	0.022±0.005	–	(4)	Centre
NGC 4051	Sy1/NL	0.06±0.01	–	0.32±0.08	0.019±0.004	–	(4)	Centre
NGC 4258	Sy1.9/L	0.10±0.01	–	0.29±0.03	0.029±0.003	–	(4)	Centre
NGC 4388	Sy2	0.03±0.01	–	0.3±0.1	0.010±0.003	–	(4)	Centre
NGC 4826	Sy2+H II	0.12±0.02	0.13±0.02	0.40±0.04	0.06±0.01	1.7±0.1	(3,6)	Centre
NGC 4945	Sy2	0.06±0.01	0.11±0.01	0.75±0.02	0.05±0.01	∼1	(27,28)	Centre
NGC 5033⋆	Sy1.8	0.12±0.01	–	0.36±0.03	0.044±0.005	∼1.9	(4)	CND[d]
NGC 5194⋆	Sy2	∼0.1-0.2	∼0.1	∼2	∼0.5	1.4±0.1	(3,7,8)	CND[d]
NGC 6951⋆	Sy2/L	–	0.13±0.02	$\gtrsim$2	$\gtrsim$2	1.4±0.1	(3,5)	CND[d]
NGC 7172	Sy2+H II	∼0.1-0.2	–	0.33±0.07	∼0.03	–	(4)	Centre
NGC 7314	Sy1.9	∼0.1-0.2	–	<0.4	∼0.05	–	(4)	Centre
NGC 7331	L	∼0.14	∼0.17	∼0.03	∼0.04	>1.7	(22,24)	Center
NGC 7582	Sy2	–	–	–	0.03±0.01	1.3±0.6	(29)	Centre
NGC 7469⋆	Sy1.2	∼0.06	∼0.05	0.95±0.1	∼0.1	∼1.4	(4,6,7)	Centre
Mrk 231††	Sy1	–	<0.03	–	∼0.2	0.72±0.09	(29,30)	Centre
Mrk 331†	Sy2+H II	–	–	–	∼0.2	∼1.3	(29)	Centre
IRAS 05414+5840†	Sy2	–	–	–	0.040±0.006	0.6±0.2	(29)	Centre
			Starbursts: $0 < T < +8$					
M82	SB+H II	∼0.03-0.1	∼0.1	∼1	∼0.2	0.7±0.1	(3,8,9)	Centre
M83	SB+H II	0.10±0.01	∼0.10±0.03	∼1	∼0.1	1.3±0.1	(23,25)	Centre
NGC 253	SB+Sy2+H II	∼0.1	∼0.1-0.3	∼0.2-1.0	∼0.05-0.3	0.8±0.1	(10,11)	Centre
IRAS 210293	SB?	0.06±0.01	0.11±0.02	–	–	–	(20)	Centre
NGC 660	SB?+Sy2/L+H II	0.07±0.01	0.05±0.01	0.7±0.3	0.05±0.02	1.0±0.3	(20,21)	Centre
NGC 891	H II	∼0.2	–	–	0.020±0.005	1.1±0.5	(29,31)	Centre
NGC 986	SB+H II	0.10±0.01	0.06±0.01	0.9±0.2	0.09±0.02	-	(20)	Centre
NGC 1808	Sy2	0.06±0.01	0.07±0.01	1.0±0.2	0.06±0.01	0.56±0.04	(20,21)	Centre
NGC 2146	SB+H II	0.08±0.01	0.10±0.01	0.8±0.2	0.06±0.01	0.77±0.05	(4,20,21)	Centre
NGC 2369†	SB?	–	–	–	0.04±0.01	1.0±0.4	(29)	Centre
NGC 2903	SB?+H II	–	–	–	0.020±0.005	0.4±0.1	(29)	Centre
NGC 3256	SB+H II	0.03±0.01	0.10±0.04	2.0±0.4	0.06±0.01	–	(20)	Centre
NGC 4355	Sy2	–	–	–	0.8±0.2	0.08±0.01	(29)	Centre
NGC 6946	SB+Sy2+H II	∼0.05-0.1	–	∼1	∼0.2	1.2±0.1	(3,4,8)	Centre
NGC 7552	SB+L+H II	0.07±0.01	0.11±0.02	1.1±0.2	0.08±0.01	0.9±0.2	(20,21)	Centre

Notes: T is the numerical Hubble type. Sources marked with a "⋆" show a particular gas chemistry with unusually high HCN/^{12}CO, HCN/^{13}CO and/or HCN/HCO$^+$ ratios; sources marked with a "†" or "††" are LIRGs and ULIRGs respectively. Values marked with a "∼" or given as a range indicate either values averaged over (or a range of values for) several positions/observations or values for which an accurate estimate of the uncertainty was not possible. [a] Sy=Seyfert; L=LINER, SB= starburst, H II=star formation bursts/H II regions, classifications taken from NED; [b] References: (1) Wild & Eckart (2000), Wild et al. (1997) and Wiklind & Combes (1997); (2) this paper; (3) Krips et al. (2008); (4) Krips et al. (2010, in prep.); (5) Petitpas & Wilson (2003); (6) Israel (2009a); (7) Israel, Tilanus & Baas (2006); (8) Paglione et al. (2001); (9) Matsushita et al. (2000); (10) Sakamoto et al. (2006); (11) Sorai et al. (2001); (12) Wilson et al. (1997); (13) Tosaki et al. (2007); (14) Brouillet et al. (2005); (15) Petitpas & Wilson (1998); (16) Bolatto et al. (2005); (17) Heikkilä et al. (1999); (18) Chin et al. (1997); (19) García-Burillo et al. (2008); (20) Aalto et al. (1995); (21) Baan et al. (2008) (and references therein); (22) Meier et al. (2008); (23) Nguyen-Q-Rieu et al. (1992); (24) Israel & Baas (1999); (25) Israel & Baas (2001); (26) Israel (2009b); (27) Henkel et al. (1994); (28) Wang et al. (2004); (29) Baan et al. (2008); (30) Glenn & Hunter (2001); (31) Sakamoto et al. (1997); (32) Wilson et al. (2008). [c] Regions in which the line ratios where determined: Centre = central $\lesssim$ 10 kpc of a galaxy; CND = circumnuclear disc, i.e. a radius < 1 kpc; GMC = average over several giant molecular clouds; SA = spiral arms. [d] Ratio determined from absorption lines. [e]Ratios determined from interferometric observations.

Table 3 – *continued*

Source	Activity Type[a]	$\frac{^{13}CO(J=1-0)}{^{12}CO(J=1-0)}$	$\frac{^{13}CO(J=2-1)}{^{12}CO(J=2-1)}$	$\frac{HCN(J=1-0)}{^{13}CO(J=1-0)}$	$\frac{HCN(J=1-0)}{^{12}CO(J=1-0)}$	$\frac{HCN(J=1-0)}{HCO^+(J=1-0)}$	Ref[a]	Region[b]
Starbursts: 0 < T < +8								
NGC 7771[†]	SB+H II	–	–	–	~0.05	~1.0	(29)	Centre
UGC 2855	?	0.08±0.02	0.11±0.01	–	–	–	(20)	Centre
IC 860[†]	H II	–	–	–	0.08±0.01	0.5±0.2	(29)	Centre
Arp 220[††]	SB+Sy2/L+H II	<0.05	~0.05	–	~0.08	0.46±0.09	(29)	Centre
IRAS 22025+4205[†]	SB?	–	–	–	0.15±0.03	0.42± 0.2	(29)	Centre
SF-spirals: 0 < T < +8								
M33	H II	~0.10	~0.14	–	–	–	(12)	GMC in SA
M31	L?	~0.13	–	~0.15	~0.02	~0.9	(13,14)	GMC in SA
Maffei 2	NONE	0.02-0.1	–	~0.4-1.3	~0.02-0.13	2.4±0.4	(22,23)	GMC in SA
Dwarf galaxies: +8 ⩽ T ⩽ +10								
IC10	SB	–	~0.1	–	–	–	(15)	GMC
LMC	NONE	~0.1	~0.2	~0.2-0.4	~0.03-0.06	~0.3-0.7	(16,17,18)	GMC
SMC	NONE	~0.1	~0.1-0.2	~0.3-0.4	~0.02	~0.4	(16,17,18)	GMC
Peculiar galaxies and/or mergers								
NGC 6240[†]	Sy2/L	~0.02	~0.01	–	~0.09	~0.8	(29)	Centre
Mrk 273[††]	Sy2/L	–	–	–	~0.2	~ 0.4	(29)	Centre
NGC 3620	SB?	–	–	–	0.08±0.03	<0.4	(29)	Centre
IC 1623[†]	?	–	–	–	0.040±0.006	1.2±0.2	(29)	Centre
Arp 55[†]	L+H II	–	<0.04	–	~0.1	~0.8	(29,32)	Centre
Arp 193[†]	L+H II	–	–	–	~0.03	~1.9	(29)	Centre
Arp 299A[†]	H II	~0.04	~0.03	~1	0.040±0.006	1.6±0.3	(29)	Centre
Arp 299B[†]	H II	~0.04	~0.03	~1	0.050±0.004	~0.8	(29)	Centre
IRAS 12112+0305[†]	L+H II	–	–	–	~0.07	~0.6	(29)	Centre
IRAS 15107+0724	H II	–	–	–	0.11±0.03	0.5±0.2	(29)	Centre

Table 4. Properties of the molecular lines detected.

Source	L_{IR} (10^9 $L_\odot$)	$L_{HCN(1-0)}$ (10^8 K km s^{-1} pc^2)	$L_{^{13}CO(1-0)}$ (10^8 K km s^{-1} pc^2)	$L_{^{12}CO(1-0)}$ (10^8 K km s^{-1} pc^2)	$M_{dense}(H_2)$ (10^8 $M_\odot$)	$M(H_2)$ (10^8 $M_\odot$)	$L_{IR}/M_{dense}(H_2)$ ($L_\odot/M_\odot$)	$L_{IR}/M(H_2)$ ($L_\odot/M_\odot$)
NGC 3032	3.9	0.03	0.08	0.8	0.3	3.8	130	10
NGC 4150	0.7	<**0.008**	0.02	0.2	<**0.08**	1.0	>**90**	7
NGC 4459	2.2	0.04	0.17	0.6	0.4	3.0	55	7
NGC 4526	5.8	0.08	0.33	1.2	0.8	5.7	72	10

Notes: L = luminosity, M = mass. The infrared luminosity (L_{IR}) is determined from the 12, 25, 60 and 100 μm fluxes using $L_{IR} = 4\pi {D_L}^2 F_{IR}[L_\odot]$, with $F_{IR}[W\ m^{-2}] = 1.8\times10^{-14}$ (13.48 $f_{14\mu m}$ + 5.16 $f_{25\mu m}$ + 2.68 $f_{60\mu m}$ + $f_{100\mu m}$) and D_L = luminosity distance. The infrared luminosities were derived from *IRAS* fluxes that were taken from the NED. The mass of the dense molecular gas is derived using $M_{dense}(H_2) = 10\ L_{HCN}\ M_\odot$ (K km s^{-1} pc^2)$^{-1}$ (Radford, Solomon & Downes 1991), while the entire molecular gas mass is derived using $M(H_2) = 4.8 \times L_{^{12}CO}\ M_\odot$ (K km s^{-1} pc^2)$^{-1}$ (Young & Scoville 1991, and references therein).

M., Goldstein M., Kaufman Z., Nantais J., Perry G., 2001, ApJS, 135, 183

Paturel G., Petit C., Prugniel P., Theureau G., Rousseau J., Brouty M., Dubois P., Cambrésy L., 2003, A&A, 412, 45

Petitpas G. R., Wilson C. D., 1998, ApJ, 496, 226

Petitpas G. R., Wilson C. D., 2003, ApJ, 587, 649

Radford S. J. E., Solomon P. M., Downes D., 1991, ApJ, 368, L15

Sage L. J., Welch G. A., 2006, ApJ, 644, 850

Sage L. J., Welch G. A., Young L. M., 2007, ApJ, 657, 232

Sakamoto K., Ho P. T. P., Iono D., Keto E. R., Mao R.-Q., Matsushita S., Peck A. B., Wiedner M. C., Wilner D. J., Zhao J.-H., 2006, ApJ, 636, 685

Sakamoto, S.; Handa, T.; Sofue, Y.; Honma, M.; Sorai, K.; 1997, ApJ, 475, 134

Sarzi M., et al., MNRAS, 2006, 366, 1151

Sarzi M., et al., MNRAS, 2010, 402, 2187

Solomon, P. M.; Downes, D.; Radford, S. J. E., 1992, ApJ, 387, L55

Sorai K., Nakai N., Kuno N., Nishiyama K., 2001, in "Galaxy Disks and Disk Galaxies", proceeding of a conference held in Rome, Italy, June 12-16, 2000 at the Pontifical Gregorian University and sponsored by the Vatican Observatory. ASP Conference Series, Vol. 230. Edited by José G. Funes, S. J. and Enrico Maria Corsini. San Francisco: Astronomical Society of the Pacific. ISBN: 1-58381-063-3, pp. 385-386

Sternberg A., Genzel R., Tacconi L., 1994, ApJL, 436, L131

Taniguchi, Y.; Ohyama, Y.; Sanders, D. B., 1999, ApJ, 522, 214

Tosaki T., Shioya Y., Kuno N., Hasegawa T., Nakanishi K., Matsushita S., Kohno K., 2007, PASJ, 59, 33

Usero A., García-Burillo S., Fuente A., Martín-Pintado J.,

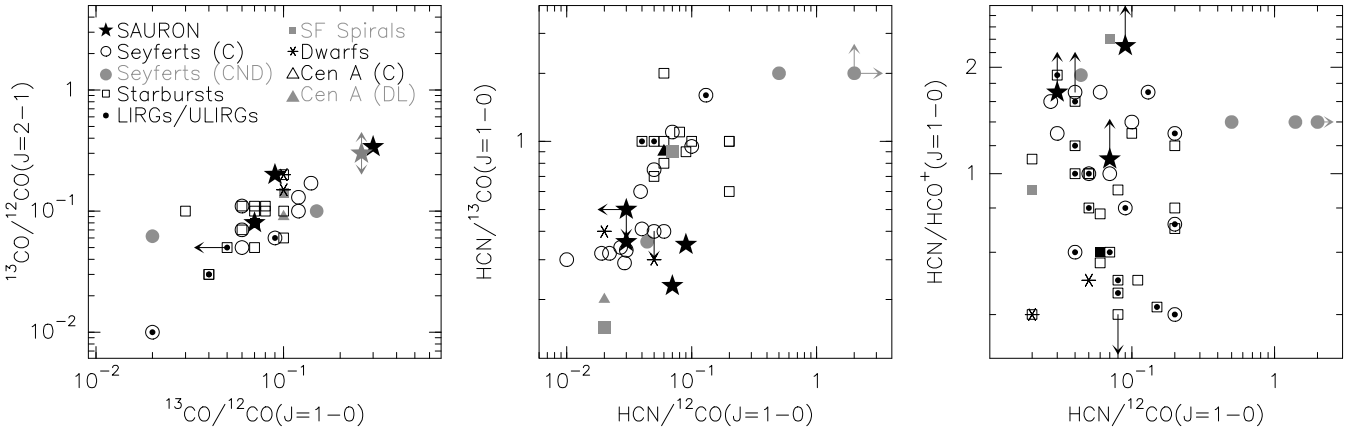

Figure 2. Molecular line ratios of the SAURON early-type galaxies compared to those of galaxies of different Hubble and activity types (see Table 3). Errors are of the order of the symbol sizes for most sources. For the labels: C = centre; CND = circumnuclear disc; DL = dust lane. LIRGs/ULIRGs are additionally highlighted by small filled circles. **Given the uncertainty of the ^{13}CO/^{12}CO(J=2–1) line ratio for NGC 4526, its corresponding symbol is plotted in grey and marked additionally with errors pointing up and down.**

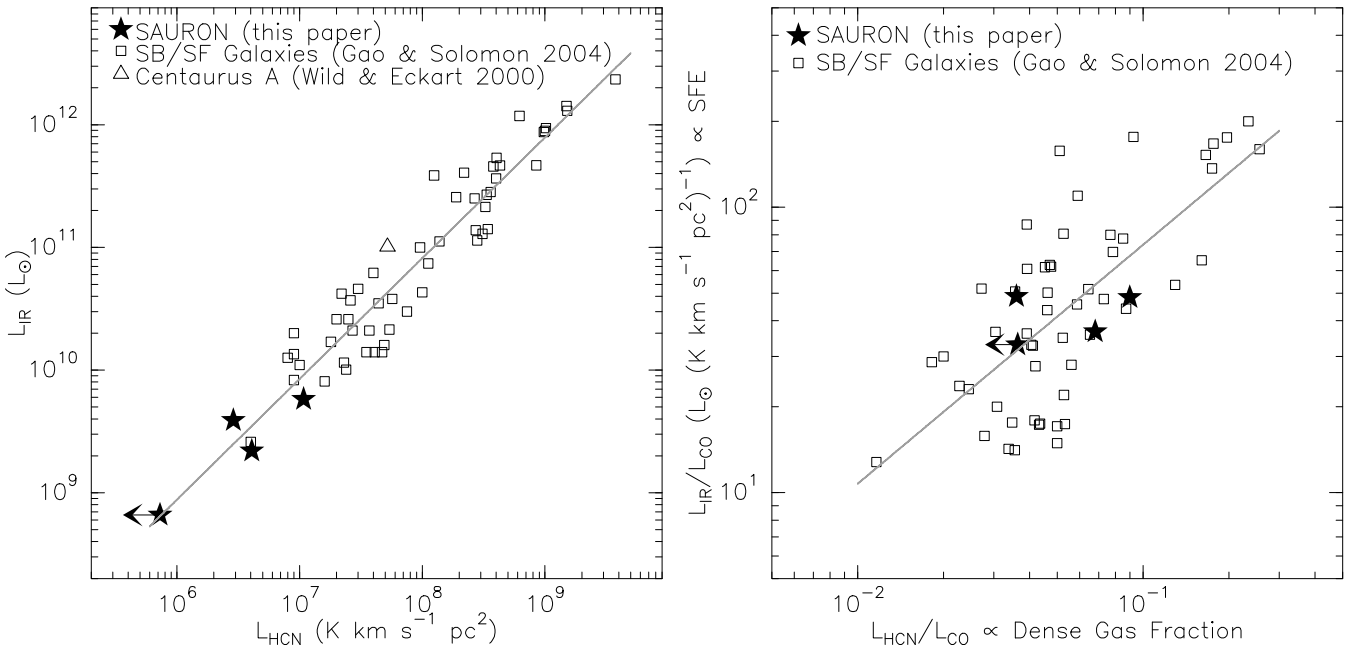

Figure 3. Infrared and HCN luminosities. *Left:* Infrared luminosity as a function of the HCN(J=1-0) luminosity. *Right:* Dense gas fraction versus star formation efficiency.

Rodríguez-Fernàndez N. J., 2004, A&A, 419, 897
Wang, M.; Henkel, C.; Chin, Y.-N.; Whiteoak, J. B.; Hunt Cunningham, M.; Mauersberger, R.; Muders, D., 2004, A&A, 422, 883
Wiklind T., Combes F., 1997, A&A, 324, 51
Wiklind T., Combes F., Henkel C., 1995, A&A, 297, 643
Wild W., Eckart A., A&A, 2000, 359, 483
Wild W., Eckart A., Wiklind T., 1997, A&A, 322, 419
Wilson, Ch.D.; Petitpas, G.R.; Iono, D.; Baker, A.J.; Peck, A.B.; Krips, M.; Warren, B.; Golding, J.; Atkinson, A.; Armus, L.; Cox, T.J.; Ho, P.; Juvela, M.; Matsushita, S.; Mihos, J.Ch.; Pihlstrom, Y.; Yun, M.S., 2008, ApJS, 178, 189
Wilson C. D., Walker C. E., Thornley M. D., 1997, ApJ, 483, 210
Yi S. K., et al., 2005, ApJ, 619, L111
Young L. M., 2002, AJ, 124, 788
Young L. M., 2005, ApJ, 634, 258
Young L. M., Bureau M., Cappellari M., 2008, ApJ, 676, 317
Young J. S., Scoville N. Z., 1991, ARA&A, 29, 581
Young L. M., et al., 2009, MNRAS, submitted
Young O., Rolaine C., Meixner M. M., Wolfire M., Tielens A. G.

G. M., Tauber J., 2000, ApJ, 540, 886